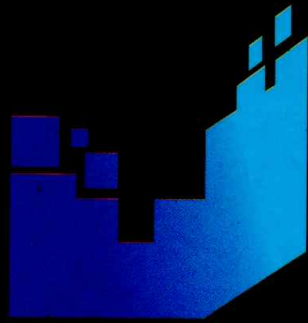




Department of Mechanical and Industrial Engineering
Faculty of Engineering Universitas Gadjah Mada



PROCEEDING

Conference on Materials

The 1st
International Conference
on Materials Engineering (ICME)
and
The 3rd
AUN/SEED-Net Regional Conference
on Materials (RCM)



AUN / SEED Net



UGM

Universitas Gadjah Mada



USM

UNIVERSITI SAINS MALAYSIA

ISBN 978-979-97986-5-7

PROCEEDING
INTERNATIONAL CONFERENCE ON MATERIALS ENGINEERING
AUN/SEED-NET REGIONAL CONFERENCE ON MATERIALS

February, 2nd – 3rd 2011
Yogyakarta, Indonesia

DEPARTMENT OF MECHANICAL AND INDUSTRIAL ENGINEERING
FACULTY OF ENGINEERING UNIVERSITAS GADJAH MADA

INTERNATIONAL CONFERENCE ON MATERIALS ENGINEERING
AUN/SEED-NET REGIONAL CONFERENCE ON MATERIALS

LIST OF CONTENT

PROCEEDING of

the 1st INTERNATIONAL CONFERENCE on MATERIALS ENGINEERING (ICME) and
the 3rd AUN/SEED-NET REGIONAL CONFERENCE on MATERIALS (RCM)

Title Page	i
Foreword	iii
List of Content.....	vii

Keynote

An Overview of Polymer-Organoclay Nanocomposites	1
Zainal Arifin MOHD ISHAK	
EAF Steel Slag Process by Slag Atomizing Technology as a Solution for Zero Waste and Green Environment	5
Hitoshi TAKAGI	
Nano-Scale Green Composites: Combination of Biomass Polymer and Cellulose Nanofiber	11
Tomoyuki NEMOTO, Rahida Wati SHARUDIN and Masahiro OHSHIMA	
Preparation of Nanocellular Foams (NCF) from Polymer Blends - NCF will provide a higher performance than conventional foams -	17
Jun KOMOTORI, Yutaka KAMEYAMA, Shoichi KIKUCHI and Yuki AMANO	
Surface Modification by Fine Particle Peening	23
Jun KOMOTORI, Yutaka KAMEYAMA, Shoichi KIKUCHI and Yuki AMANO	
Work-softening, high pressure phase formation and powder consolidation by HPT	29
Minoru UMEMOTO	

Biomaterials

3D-porous calcium phosphate cement from α-tricalcium phosphate (α-TCP) spheres for bone tissue regeneration	33
Pham TRUNG KIEN, Michito MARUTA, Kanji TSURU, Giichiro KAWACHI, Shigeaki MATSUYA and Kunio ISHIKAWA	
A novel bioartificial pancreas for xenotransplantation	37
Nguyen M. LUAN, Yuji TERAMURA and Hiroo IWATA	
Development and Characterization of Al₂O₃/Bovine Hydroxyapatite	43
M.K. Herliansyah, M. Waziz Wildan, Suyitno, Punto Dewo	

Effect of a Novel Sintering on Physical and Mechanical Properties Of Carbonated Hydroxyapatite Ceramics	51
Yanny-Marliana, B.I and Ahmad-Fauzi M.N	
Effect of Cold Deformation and Sandblasting on Tensile Strength and Corrosion Resistance of AISI 316L	57
Suyitno and TeguhDwi WIDODO	
Influences of Chitosan Addition to Morphology of Yttrium Stabilized Zirconia (YSZ) Nanoparticle for Dental Bridge Application	61
Heru HERMAWAN, Bambang SUNENDAR	
Manufacturing Processes of Bone Screws for Orthopaedic Implant By Conventional Lathe Machine	65
PringgoWidyo LAKSONO, Muslim MAHARDIKA, SUYITNO, Punto DEWO, GunawanSetia PRIHANDANA, UripAgus SALIM, Budi ARIFVIANTO	
Natural Hydroxyapatite: A Comparative Study of Bovine Hydroxyapatite, Calcite Hydroxyapatite and Gypsum Hydroxyapatit	71
M. K. Herliansyah, M. W. Wildan, A. E.Tontowi, Suyitno, PuntoDewo	
Surface Structure of AISI 316L after Sandblasting and Surface Mechanical Attrition Treatment	79
B. ARIFVIANTO, M. MAHARDIKA, SUYITNO	
Ceramics	
Activation of Natural Zeolite as Water Adsorbent for Mixed-Adsorption Drying	85
Mohamad DJAENI, Laeli KURNIASARI, Aprilina PURBASARI, Setia Budi SASONGKO	
Electrical Characteristic Of Fe₂O₃ Thick Film Ceramics Made From Local Mineral In Air And Ethanol Atmosphere	89
Endi SUHENDI, Hera NOVIA and DaniGustaman SYARIF	
Estimating the Thermal Conductivity of Nanoclay Using theHasselman and Johnson Model	91
Lawrence V. MADRIAGA, Emee Grace D. TABARES, Ivy Ann C. RAZONADO and Leslie Joy L. DIAZ	
Fabrication of MgAl₂O₄-CeO₂ Ceramics as Simulated Inert Matrix Fuel (IMF)	95
DaniGustaman SYARIF	
Incorporating High Molecular Weight Chitosan into Natural Clay for Potential Biodegradable Food Packaging Material	99
Indriana KARTINI, Nurul H. APRILITA, Tutik D. WAHYUNINGSIH, Eko S. KUNARTI, Endang RAHAYU and Ajeng P. MARHAENI	

Indium Tin Oxide Surface Properties Study by Means Of XPS	105
Bagas PUJILAKSONO	
Mesoporous Carbon Gel as a Support for Palladium	123
U. Kijisrichareanchai, M. Sukwattanasinitt, J. Panpranot, N. Tonanon , T. Charinpanitkul	
Preparation of Adsorbent from Bagasse Fly Ash (BFA) for Removal of Cu (II) and Ni (II) and The Application	127
Avissa YUNITA, Esti T. WIDYASTUTI, Agus PRASETYA	
Study Of Biosynthesis Silica Nanoparticles From Husk Use FusariumOxysporum	133
YUSMANIAR, Soegijono B., Ambarsari LAKSMI, Elizabeth R. IRMA	
The Effect of CaCO₃ Addition on the Crystallization Behavior of ZnO Crystal Glaze Fired at Different Gloss Firing Temperatures	137
Abdul Rashid JAMALUDIN, Shah Rizal KASIM, ZainalArifin AHMAD	
The Effect of NaA Zeolite Modification on The Characteristics of Polyacrylamide – NaA Zeolite Pervaporation Membranes	143
Kris Tri BASUKI, Deni SWANTOMO, Christina Aprilliani PASKALIN	
The Effect of Thermal Shock on Bending Strength of Zirconia Ceramics	147
Muhammad W. WILDAN, B. Setyoko, Suhanan and Heru SB. Rochardjo	
The Infrared Absorption Spectral Changes Of Coconut Shell Carbon With Polyvinyl Alcohol Stimulant	153
Meytij Jeanne Rampe, BambangSetiaji, WegaTrisunaryanti and Triyono	

Composites

A Review Study on the Adhesively Bonded Composite Lap Joint in Aerospace Industry	159
S.N. ABDUL RAZAK, A.R. OTHMAN	
Deposition and Characterization of Chrome Carbide Based Ceramic Matrix Composite Coatings By High Velocity Oxygen Fuel Thermal Spray Coating	165
Budi PRAWARA, Edy RIYANTO, Budi PRIYONO	
Effects of Plate Thickness on Bullet Resistability of Ramie Fiber Composite	169
Heru S.B. ROCHARDJO, Rini DHARMASTITI, M. Waziz WILDAN and SUPARYONO	
Hygrothermal Aging Studies on Biodegradable Poly(butylene succinate)/ Organo-montmorilloniteNanocomposites	173
Yi Jing PHUA, ZainalArifin MOHD ISHAK, Wen Shyang CHOW	

Mechanical and Thermal Properties of Reprocessed Kenaf Fibre-Filled-Poly(butylene succinate) Composites	177
J.M. LEE, Z.A. MOHD ISHAK	
Microstructure and Properties of Open Air Hot Pressed Al/SiCp Composites	183
T. MUSTIKA, B. SOEGİYONO and I.N. JUJUR	
Minimizing Property Variation in Natural Fiber Reinforcements for Green Composite Materials Applications	187
Leslie Joy L. DIAZ, Stela Marie HAGAD and Peter June M. SANTIAGO	
Polymeric Thermoplastic Composite Bipolar Plate for PEM Fuel Cell	195
EniyaListiani DEWI and DewiKusuma ARTI	
Sinter Process of SiC Nanoparticles Reinforced Aluminium Metal Matrix Nanocomposites	199
Koswara, B. SOEGIJONO, Dedi PRIADI	
Strength of Timbers: A Case Study in Cambodia	203
CHHOUK ChhayHorng	
Study on Mechanical Properties of Clay Reinforced Epoxy Nanocomposites	211
Kusmono, Z.A. MOHD ISHAK, Angga ZURAHMAN	
Synthesis and Thermal Characterization of Elastomer Polyurethane/Clay Nanocomposites	215
Teuku RIHAYAT and SURYANI	
Tensile and Electrical Properties of Injection Molded Short Glass Fiber and Short Carbon Fiber Reinforced Polycarbonate Hybrid Composites	219
T.T.LAW, Z.A. Mohd ISHAK	
Tensile Properties of Pineapple Leaf Fibre (PALF) Reinforced High Impact Polystyrene Composites: Effect of Crosslinking Agent and Electron Beam Irradiation	225
J.P SIREGAR, E.H. AGUNG, S.M SAPUAN and T. CIONITA	
The Growth of Inorganic Nanoparticles and Organic Matrix Entrapment in the Thermally Annealed and Post-Hydrothermally Treated TiO₂-Polymethyl Methacrylate Nanocomposites Derived From Sol-Gel Process	227
Akhmad Herman YUWONO and John WANG	
The Influence of Wood Powder Adding on the Porosity of Composite Material	233
Sutrisno, Arif TJAHOJONO	
The Particle Board Made of Rice Husk as Thermal Isolator For Ceiling	237
Khairul MUHAJIR	

The Testing of Internal Bond Strength of Particle Board Made of Rice Husk	243
Khairul MUHAJIR, Toto RUSIANTO, Rizqi FITRI	

Failure Analysis

Failure Analysis of VRU (Vapor Recovery Unit) Discharge Silencer	247
Beny BANDANADAJA, Wiwik PURWADI and M. ACHYARSYAH	
Failure Analysis on a Ruptured Dampener	251
Hermawan JUDAWISASTRA, Slameto WIRYOLUKITO	
Failure Analysis on Copper Brass Radiator Leakage on TBR 541 MPV	257
Tono SUKARNOTO, Supriyadi	
Failure Characterization of Polypropylene Thermoplastic Honeycomb Core Subjected to Low Velocity Impact	261
Amie NorFreedda AMIR, A. R OTHMAN	

Metals

A Study on the Low Rotational Speed For the Joining Between YSZ-Alumina Composite and 6061 Aluminium Alloy By Friction Welding	267
Uday M. B., M.N. Ahmad Fauzi, Zuhailawati H., A.B. Ismail	
Analysis of FSW Welds Made of Aluminum Alloy 6110	273
Jarot WIJAYANTO, Sudarsono, and Rizqi FITRI	
Barium Titanate Nanoparticles: Synthesis, Characterization, Properties	277
Kyaw NAING, Thandar WIN, and Khin Mar TUN	
Breakaway Oxidation of FeCr System (Fe-2.25Cr, Fe-10Cr, Fe-18Cr and Fe-25Cr) In O₂ and In O₂ + H₂O Environment at 600°C	283
Bagas PUJILAKSONO	
Dissolution of MnS Inclusions of Stainless Steel under Cyclic Voltammetry in Chloride Solution	309
Sri Hastuty, Atsushi NISHIKATA, and Tooru TSURU	
DSC Analysis of Cu-Zn-Sn Shape Memory Alloy Fabricated by Electrodeposition of Tin on Brass	313
Richard DV. ESPIRITU and Alberto V. AMORSOLO	
Effect of Chromium Content on Isothermal Oxidation Behavior of Zr-Nb Alloys at High Temperature	317
DjokoHadi PRAJITNO	

Effect of Mg₂Si on Electrochemical Behavior Al-Mg-Si Heat Treated PVD Coatings	323
Hariyanti, Gamal A. EL-MAHDY, Atsushi NISHIKATA and Tooru TSURU	
Effect of Powder of Copper As A Makeup Material on The Hardness of Base Metal	327
Dody PRAYITNO, Achmad HALIM	
Effect of Preheating on Fatigue Crack Growth Rate Behaviour of Friction Stir Aluminium Alloy 6061-T6 Welds	335
MochammadNoerllman, SckolastikaNinien	
Effects of Mixing Method on Properties of Cu-NbC Composites Fabricated via Powder Metallurgy	343
Zuhailawati HUSSAIN, Radzali OTHMAN, Bui D. LONG, Minoru UMEMOTO	
Environmentally – Assisted Crack Growth in Deaerator Storage Vessel Steels	347
Erwin SIAHAAN	
Evaluation of Halogen Free Flux on IMC Formation and Reliability of SAC/NiP Solder Joint	353
Nurulakmal M. SHARIF, Boon Pin, CHAN, and Wan Koon, OOI	
Hydrogen Storage Properties of the Mg-Ni Alloy Containing 5 wt% Ti and Mg-Ti Alloys Containing 5 wt% Al and 10 wt% Fe Prepared by Mechanical Alloying	357
Hadi SUWARNO	
Influence of Chitosan Molecular Weight on Adhesive and Bioactivity Properties of Ti-6Al-4V Coating	363
Hermawan JUDAWISASTRA, Jamillah B.A. NORDIN, Bambang SUNENDAR	
Modification of Silicon in Hypereutectic Aluminum Silicon Alloys	369
Nguyen H. DUNG, Nguyen H. HAI, Tran D. HUY, Nguyen V. THAI	
Nitrogen Implantation Effect on Hardness and Corrosion Rate of 304 Stainless Steel	375
Viktor MALAU and Kusmono	
Plasma Nitriding Effects on Hardness and Corrosion rate of 304 Stainless Steel	381
Viktor MALAU	
Preparation of Al-Ti-B Master Alloys from Titanium Oxide and Boric Acid	387
Huynh Cong KHANH, Pham Van CUONG	
Preparation of Aluminium Nano Powder by High Energy Milling Attrition	393
NweNwe SOE, PhyuPhyu WIN	

Study of Carbon Diffusion Thickness of AISI 3115 Affected by Heating Temperature and Andong's Bamboo Charcoal Grain Size on Pack Carburizing	397
PutuHadi SETYARINI, NinisNing RATRI, WinarnoYahdi ATMODOJO	
The Effect of Al₂O₃, ZnO and Cr₂O₃ Fluxes in A-TIG (Active flux-TIG) Welding on AISI 316L Stainless Steel	401
Slameto WIRYOLUKITO, Restu SIHOTANG and Surasno	
The Effect of Groove Dimension on Panel to the Damping Characteristics of the Panel	407
Sunardi, I Made MIASA, R. SOEKRISNO	
The Influence of NiAl Particle Size on Impact Resistance of HVOF Thermal Sprayed Cr₃C₂-NiAl-Al₂O₃ Coating	413
Asyraf H. RASFA, Husaini ARDY and Budi PRAWARA	
The Kinetics of Blood Cockle Shell and East African Land Snail Shell as Pack Carburization Energizers for Surface Hardening of Low Carbon Steel	417
Budi Hartono SETIAMARGA, AndhikaYusPratama TAMBUNAN and Umen RUMENDI	
The Mercury Corrosion Attack on Stainless Steel Material at Top Side Gas Wells Facility	421
ArdianNengkoda, Supranto	
To Reduce the Fracture Mechanic at the Welding Spiral Pipe with Stress Relief Annealing	427
Nur SUBEKI, M Jufri and Lukman HZ	
Wear Resistance of High Velocity Oxygen Fuel Sprayed Cr₃C₂-NiAl-Al₂O₃ Coatings	435
Edy RIYANTO, Budi PRAWARA, Asyraf H. RASFA	
Polymers	
Adsorption Isotherm of Mesoporous Biphényl-bridged Organosilica Material	441
Eduardo R. MAGDALUYO, Jr., Raymond V. RIVERA-VIRTUDAZO and Emily V. CASTRICIONES	
Influences of Polysiloxane with Phenyl Group on The Optical and Mechanical Properties of Polybenzoxazine-Polysiloxane Hybrids	443
Hosta ARDHYANANTA, Moh. FARID and Tsutomu TAKEICHI	
Irradiation Grafting Of Hydrophilic Monomer Onto Chitin For Ion Exchange Application	447
GatotTrimulyadi REKSO	

Parametric Study of the Surface Modification of Polyimide Films by Plasma Treatment in an Ion Shower Facility.....	453
Alberto AMORSOLO, JR., Jose Cornelio FLORES, Eric MIRANDA, Krisette Anne DE CHAVEZ, Jeremiah CHAN, Bryant LANIOG, Anna Monica DIPASUPIL and Henry RAMOS	
Prototype Cryogenic Recycling Machine for Scrap Automobile Tire Peel.....	459
Mon David PAKINGAN, John Henri RUIZOL, Juan Rodrigo FONSECA, Philip Ellison CERVEZA and Homer CO	
Study of Effect Ammonium Persulfate and Amino-Methyl-propanol in grafting Maleic Anhydride on Polietilene in the Making Softener.....	461
Nurudin BUDIMAN, Sugeng, Melya D.SEYAYANG	
Synthesis and Studies on the Effect of Phenyl side –chain content on Refractive Index of Polysiloxane Resin.....	467
Rafiza RAMLI, Ng Chee MANG, Zulkifli AHMAD, Mariatti JAAFAR	
The Effect of Mastication Process to Curing Characteristic, Mooney viscosity, and Physical Properties of Natural Rubber.....	473
Abu HASAN, Rochmadi, Hary SULISTYO, and Suharto HONGGOKUSUMO	
Viscometric Flows for Complex Viscoelastic Flows in Cross-Slot Devices.....	479
Bumroong PUANGKIRD	
Semiconductor	
Effect of Calcination Temperatures on the Properties of Dip-Coated Barium Ferrite Thin Films.....	483
A.A. GERRY and A. NURUDDIN	
Electropolymerization of Pyrrole in Aqueous Solution on Carbon Electrodes for Ion Phosphate Sensor.....	487
Robeth V. MANURUNG, Totok M.S SOEGANDI and Hiskia	
Formation of CuAlO₂ Films by Ultrasonic Spray Pyrolysis.....	491
Iping SUHARIADI, Zainovia LOCKMAN, SabarDerita HUTAGALUNG, Kamsul ABRAHA, Atsunori MATSUDA	
Microwave Induced Irradiation of Barium Ferrite Prepared by Sol-gel Auto-combustion.....	495
A. NURUDDIN, R. RIADY and SUYATMAN	
Response of Organic Semiconductor Thin Film Copper Phthalocyanine to Vehicle Gas Emission at Room Temperature.....	499
La ABA, I Nyoman SUDIANA, Kuwat TRIYANA, Yusril YUSUF, M. Iqbal BARATA	
Structural and Magnetic Properties of Co-Milled of Nd₂Fe₁₄B and Fe₃Si Powders.....	503
E. Handoko	

To Reduce the Fracture Mechanic at the Welding Spiral Pipe with Stress Relief Annealing

Nur SUBEKI^{1*}, M Jufri² and Lukman HZ³

¹Mechanical Engineering Department, University of Muhammadiyah Malang, East Java, Indonesia

²Mechanical Engineering Department, University of Muhammadiyah Malang, East Java, Indonesia

³Mechanical Engineering Department, University of Muhammadiyah Malang, East Java, Indonesia

Abstract: Submerged Arc Welding (SAW) is a welding process used for fabrication of pipes, for example spiral welded pipes. The technique can be operated automatically and has a high reliability in many various welding applications. Some factor affecting the strength of weld metals are heat input, current, and chemical composition of filler, flux, and base metal and also treatment after welded. The present investigation aims to study fracture mechanic after treatment with Stress Relief Annealing on submerged arc spiral welded steel pipes. Material used in this experiment was API 5L X-65 for spiral welded steel pipes. Welding was carried out using voltage of 35 volt, welding speed of 13,67 mm/s whereas post weld heat treatment temperature namely standard, 500°C, 600°C, 700°C to reduce fracture mechanic. Results show that, the annealing temperature while to height reducing fracture mechanic start with annealing temperature at 500°C, and decrease in 600°C, 700°C and without annealing.

Key Words: SAW (Submerged Arc Welding), spiral pipes, heat treatment, fracture mechanic.

1. INTRODUCTION

Steel pipe API 5L X65 is a pipe manufactured and produced based on API (American Petroleum Institute) standard. This pipe has carbon of 0,26 %; it is classified in low carbon. This type of pipe is usually manufactured by using Submerged Arc Welding (SAW). The problem commonly occurs in SAW (Submerged Arc Welding) API 5L X65 steel pipe is caused by the rate of high cooling in welding; it includes the emergence of residual tension and forming of microstructure in the form of martensit, residual austenite and carbide that declines toughness and strong of welding so that causes crack. If dynamical load occurs in welding connection, then crack will quickly creep and causes fracture. To solve this problem, treatment for stress relief annealing will be useful in impeding the rate of creeping in fatigue crack on the result of welding (SAW) API 5L X65 steel pipe.

2. REVIEW OF RELATED LITERATURE

2.1. Steel

Steel can be defined as a mixture from iron and carbon where carbon substance (C) is being the base of mixture. Besides, steel also contains other substances like sulfur (S), phosphor (P), silicon (Si) and manganese (Mg) in limited number.

2.4 SAW welding

SAW (Submerged Arc Welding) process is known by term of submerged arc welding. The basic principle of this welding uses electrical current to produce arc (arc) so

According to Eunorom, steel is a compound from iron carbon and other substance where the carbon scarcely more than 2% (Vliet dan Both, 1987).

2.2. Steel Carbon

Steel carbon is compound between iron and carbon with little Si, Mn, P, S and Cu. The nature of carbon depends on carbon in the steel.

Steel carbon is classified based on carbon contain, strength and toughness. Steel carbon consists of three substance; they are:

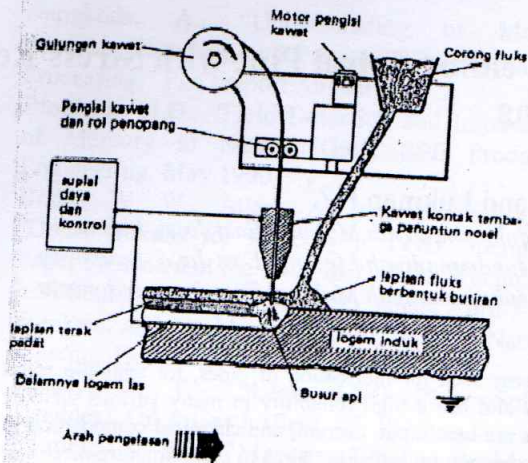
- Low steel carbon ($C < 0,2\%$)
- Medium steel carbon ($0,2\% < C < 0,5\%$)
- High steel carbon ($0,5\% < C < 1,7\%$)

2.3. API 5L X 65 Steel Pipe

API 5L X65 steel pipe is a pipe manufactured and produced based on API (American Petroleum Institute) standard. API 5L X65 steel pipe by specification of 5L is standardized specification by conference of making and distribution of line pipe for oil, water and gas by special usage.

Chemical composition of API 5L X65 steel pipe is C=0,1%, Mn=1,2%, Si=0,2%, P=0,015%, S=0,08%, Al=0,035%, Nb=0,03%, V=0,05% or $C_{max}=0,26\%$, $Mn_{max}=1,4\%$, $P_{max}=0,03\%$, $S_{max}=0,03\%$. API 5L X65 steel pipe has minimum mould strength of 448 Mpa and minimum tensile strength is 530 Mpa (Mittal Steel South Africa data, 1995).

that it can melt filler wire. In this SAW welding, filler wire is submerged in flux so that it can form enough strong of slag to protect filler wire to cool (Sonawan, 2003). SAW scheme is illustrated in Picture 1.



Picture 1. SAW scheme

The example SAW welding application is pipe welding (whether it is from longitudinal or round pipe), industry of ship, welding for huge tank and surfacing and cladding.

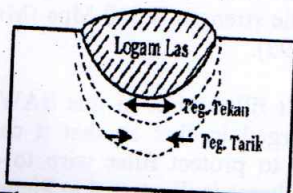
2.5. Structure of micro welding

The mechanical nature of welding connection that includes tensile strength, toughness and strength toward the rate of fatigue crack on steel depends on microstructure in welding. According to Abson and Pargeter (1986), welding mikrostruktur consists of two combination or more of the following phase:

1. Ferrite grain limitation formed on the temperature between 1000° up to 650°C on austenite grain limitation.
2. Ferrite Widmanstätten, formed on grain and grow in the middle of austenite grain in parallel plates. This ferrite formed in temperature interval of 750° up to 650°C .
3. Acicular ferrite formed under 650°C in austenite grain and formed (lath) that is arranged traverse like plait. (interlocking structure).
4. Bainite, formed on temperature of 500°C in lath.
5. Microconstituent (martensite or residual carbide) in very little number.

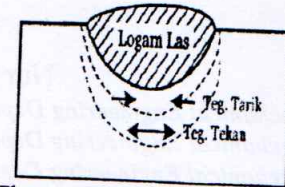
2.6. Residual Stress

During welding, an area under welding metal will in expansion, while under this try to hold it. The expansion area will have press strength will the under opposes with tensile strength, like illustrated in Picture 2.



Picture 2. The condition of tensile during heating

In contrast, during cooling process, the area under the welding metal experience tensile strength and area under it oppose by press like illustrated in Picture 3.



Picture 3. The condition of tensile during cooling

Tensile in welded plates will still exist up to base temperature. This tensile called as residual stress. If residual tensile is tensile strength, then it would be danger for welding construction, because if this tensile strength higher in such area (S_U), then it can cause crack up to the surface of welding metal.

2.7. Stress Relief Annealing

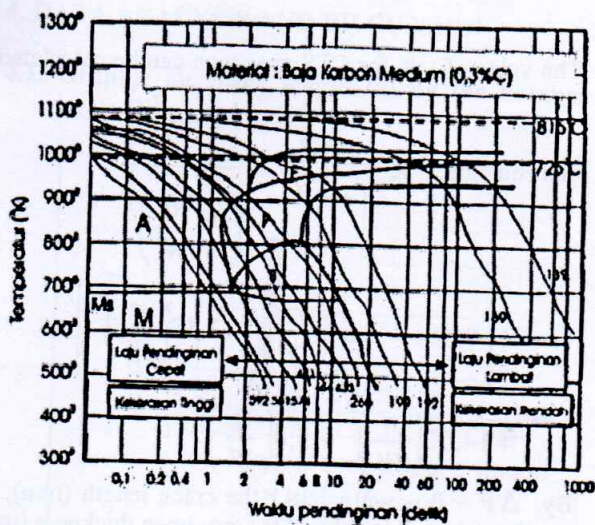
Stress relief process is a process of heat treatment after welding or post weld heat treatment (PWHT) that is aimed to eliminate residual tensile and microstructure in the form of martensite, residual austenite and carbide that is emerged in welding process. So that, it can increase toughness, strength, welding toughness and HAZ also increase endurance toward corrosion or even the rate of fatigue crack creeping.

Stress relief on steel usually conducted by heating in interval temperature of 450° up to 700°C , cooling time between 1 up to 3 hours and the rate of cooling is 1° up to 5°C/minute (Radaj, 1992).

Annealing is aimed to soften steel so that it is easier to be manufactured by machine in cool condition, soften crystal and eliminate tensile. On this process, steel is heated slowly under the submerged temperature. Temperature depends on the type of steel in (0,5-2) hours, it is continued by cooling it in special chamber of this heat or by submerging workspace in lime powder, dust, fine sand, or other substance that can decelerate cooling process.

2.8. CCT Diagram

Commonly, microstructure on steel depends on the cooling speed from the temperature of austenite up to base temperature. Because of the change in this structure then the mechanical nature owned by material will change. The correlation between cooling speed and microstructure usually show in diagram that correlates temperature (T) and time (t), transformation temperature is CCT diagram (Continuous Cooling Transformation). CCT diagram illustrated in Picture 4.



Picture 4. CCT Diagram

This diagram is not only observe the correlation between temperature and time, but also phases that possibly occurs in cooling case. A in phase diagram of Austenite, F = Ferrite, P = Perlit, B = Bainit, M = Martensit and Ms (Martensit start) = transformation line from martensit phase. While the numbers in every cooling line state the toughness number (Sonawan, 2003).

Microstructure in welding metal and HAZ are also influenced by cooling speed. It is caused by the cooling process of liquid metal (solidification) and transformation phase that is very sensitive toward cooling speed. As the example of cooling speed on steel is it will cause the form of micro in the form of hard and brittle martensit (Subekhi, 2005).

2.9. Fatigue

Fatigue is creeping process because of periodical dynamical load. The main cause of fatigue failure is crack creeping. For component or structure by load that fluctuates during operation, fatigue failure is the main factor that should be considered to determine the limit of planning tensile because almost 90% of failure or concentration failure is always caused by repetition load or fatigue fracture (Broek, 1987).

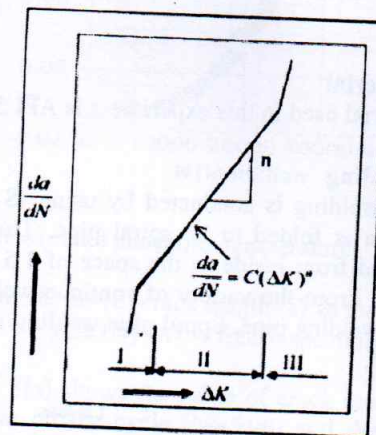
The main concept of fracture mechanic is a construction that is not should be 100% without defect but can have defect by defect time requirement (failure) that can be predicted fast.

Crack creeping on steel plates is influenced by many factors; they are plate thickness, plates material or product type, manufactured process, heat treatment, cool deformation and environment (Broek, 1987). Besides, crack creeping also influenced by residual tensile. Residual tensile on surface is driving tensile that increase endurance toward crack, while residual tensile inside is residual tensile strength that accelerate crack creeping.

Fatigue failure process can be divided into three steps; they are:

- a. Oscillating deformation

- b. Crack, whether it is on the surface or even defect on workspace.
- c. Crack creeping that will cause fatigue crack. The rate of crack creeping ($\frac{da}{dN}$) as the function of ΔK is illustrated in Picture 5.



Picture 5. The characteristic of crack fatigue (Broek, 1987)

From Picture 2.5, it can be seen that the characteristic of crack fatigue can be divided into three areas:

- a. Area I
It is called as fatigue treshold.
- b. Area II
In this area, the crack creeps linearly so that it is still considered in structure planning. In this area, there is Paris law (Broek, 1987) :

$$\frac{da}{dN} = C(\Delta K)^n$$

Where n is slope from curve and C is coefficient.

- c. Area III
This area is ignored in structure planning because the rate of creeping very fast so that difficult to control. The number of ΔK is factor difference of intensity from maximum strains that can be wrote as follow:

$$\begin{aligned} \Delta K &= K_{max} - K_{min} \\ &= Y \Delta \sigma \sqrt{\pi \times a} \\ &= Y(\sigma_{max} - \sigma_{min}) \sqrt{\pi \times a} \end{aligned}$$

Where,

ΔK : is stress intensity factor range on the end of crack, a : the length of crack, σ = tensile and Y : is parameter that depends on (1) crack and (2) the size and the geometry of specimen.

3. METHODOLOGY

3.1. Research

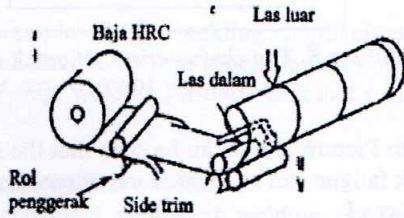
This research is experiment and literary study. It is by having experiment, observation and directly study on subject.

3.2. Material

Material used in this experiment is API 5L X65 steel.

3.3. Welding

The welding is conducted by using (SAW). Plate in coil form is folded to be spiral pipe. Then, welding is conducted from inside in the space of 1,5 meter outside the pipe. From the variety of continue welding model is outside welding pipe. Spiral pipe welding is illustrated in Picture 6.



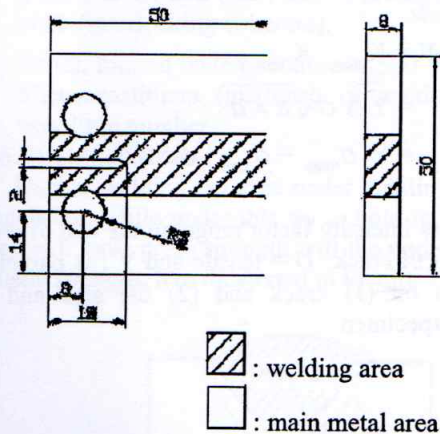
Picture 6. Spiral welding pipe

3.4. Stress Relief Annealing treatment

In this process, welding connection of API 5L X65 steel pipe is heated (stress relief) in heating chamber by temperature of 500⁰ C, 600⁰ C and 700⁰ C by 60 minutes. Then, it is cooled slowly (annealing) by air media.

3.5. Creeping testing of fatigue crack

Fatigue testing is conducted by tensile frequency of 5-15 Hz, tensile level of 40% from melted tensile and stress ratio 0,5. Specimen used here is based on ASTM E 647-95a in the form of compact tension specimen (CTS) like in the Picture 7.



Picture 7. Specimen by CTS form (Standard ASTM E 647-95a)

The value of K for CTS specimen can be calculated by

$$\text{this equation: } K = \frac{\Delta P}{B\sqrt{W}} \times \frac{\left(2 + \frac{a}{W}\right)}{\left(1 - \frac{a}{W}\right)^{\frac{3}{2}}} \times \left[0,866 + 4,64\left(\frac{a}{W}\right) - 13,32\left(\frac{a}{W}\right)^2 \right] + 14,72\left(\frac{a}{W}\right)^2 - 5,6\left(\frac{a}{W}\right)^4$$

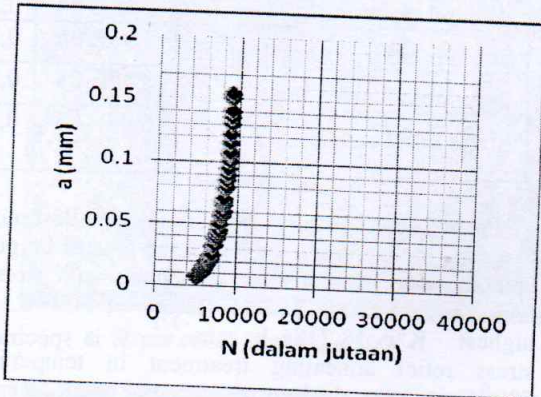
By, $\Delta P = P_{\max} - P_{\min}$, a : the crack length (mm), W : specimen length (mm) and B : specimen thickness (mm).

3.6. Fraktografi observation

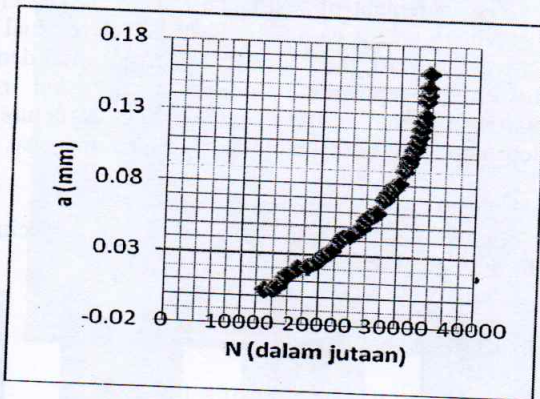
Fraktografi observation (fracture) of fatigue crack in welding area uses scanning electron microscope (SEM) that is equipped with energy dispersive X-ray (EDX) spectrometer.

4. DATA ANALYSIS AND DISCUSSION

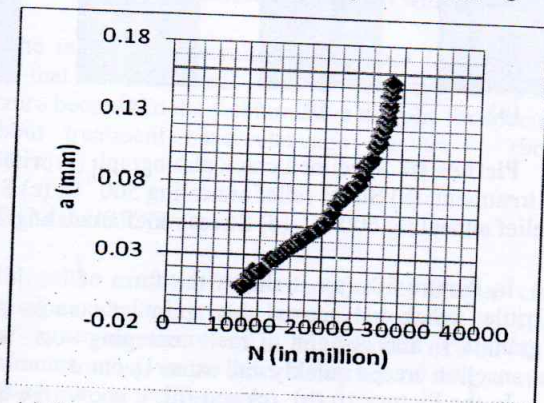
4.1. Graphic on crack length (a) by the number of cycle (N)



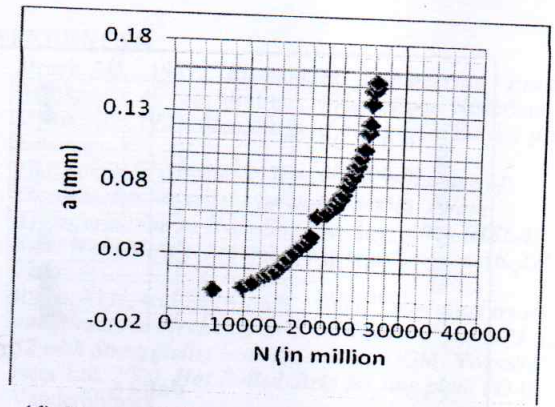
(a) without treatment



(b) Stress relief annealing temperature 500 °C



(c) Stress relief annealing temperature 600 °C



(d) Stress relief annealing temperatures 700 °C

Graphic 8. (a)-(d) crack length (a) vs the number of cycle (N) on the fourth specimen

Graphic 8(a) shows the value of crack creeping (a) it is 0,007 mm on the cycle (N) 5140 and the last crack creeping (a) is 0,154 mm on cycle (N) 9019.

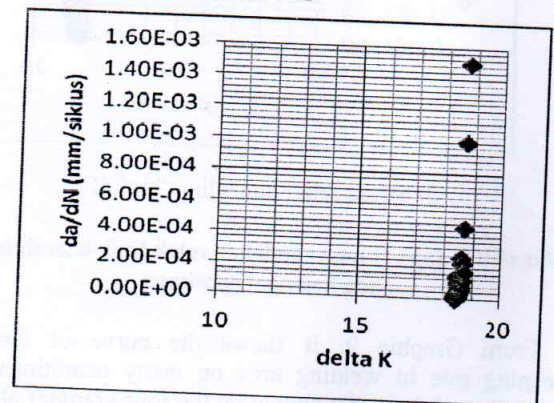
Graphic 8. (b) show the value of beginning creeping (a) it is 0,004 mm on cycle (N) 13032 and the last crack creeping (a) is 0,16 mm on cycle (N) 33660.

Graphic 8. (c) shows the value of beginning crack creeping (a) of 0,005 mm on cycle (N) 5729 and the last crack creeping (a) is 0,153 mm on cycle (N) 26279.

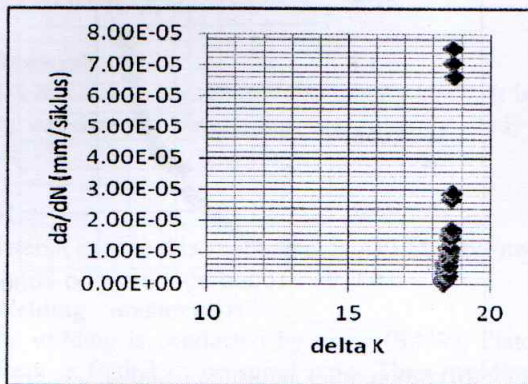
Graphic 8. (d) shows the value of beginning crack creeping (a) it is 0,008 mm on the cycle (N) 9712 and the last crack creeping (a) is 0,154 mm on the cycle (N) 28436.

From graphics 8. (a), (b), (c) and (d), it can be found the graphic by the most number of cycle (N) of 33660 on stress relief annealing treatment in temperature 500 °C. It means that on stress relief annealing treatment in 500 °C can give the best crack resistance than in the number of cycle without treatment of by stress relief annealing treatment in temperature 600 °C and 700 °C.

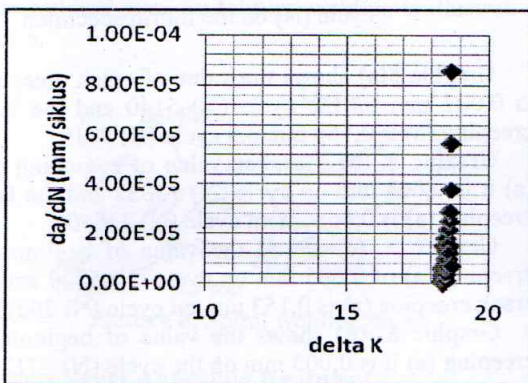
4.2. Graphic da/dN with K



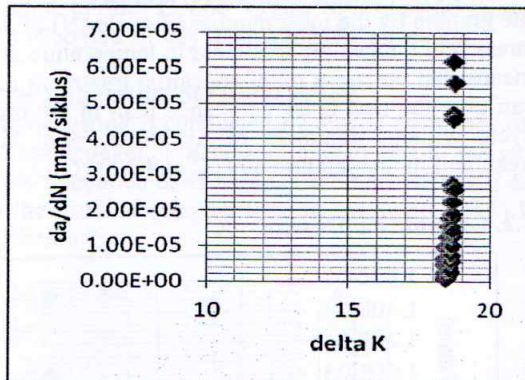
(a) Without treatment



(b) Stress relief annealing 500⁰ C



(c) Stress relief annealing 600⁰ C



(d) Stress relief annealing 700⁰ C

Grafik 9. (a)-(d) Laju rambatan retak fatik daerah las pada keempat spesimen

From Graphic 9. it shows the curve of fatigue creeping rate in welding area on many conditions. In linear part of the curve shown by the four graphics above is the area where the rate of creeping follows the Paris law so that by making trendline linier on this area, it can be found exponential value of n and C constant for Paris law. The value of n and C from each is illustrated on the Table1.

Table 1. Paris Constant from the four specimens

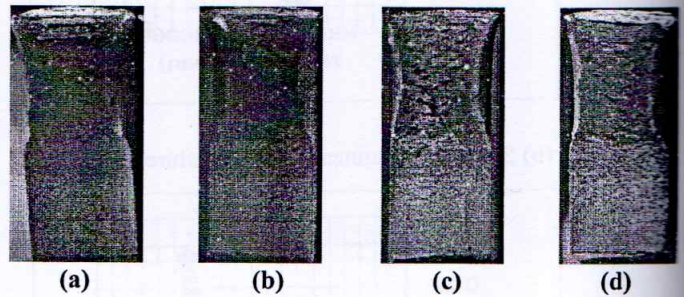
SPECIMEN	C mm/siklus	n
Without treatment	2,62E-04	0,2739
Stress relief annealing 500 ⁰ C	2,96E-05	0,2590
Stress relief annealing 600 ⁰ C	8,49E-05	0,2846
Stress relief annealing 700 ⁰ C	6,09E-05	0,2718

From Table 1. can be seen that the smallest number of C means the increment of resistance toward fatigue crack creeping rate occurs in the specimen with stress relief annealing treatment in temperature of 500⁰ C. For the highest K is 18,7186 kg.mm^{-3/2}; it is specimen with stress relief annealing treatment in temperature of 500⁰ C; it shows the best resistance of crack creeping rate by accelerated value of smallest n 0,259.

The increment of resistance toward fatigue creeping on welding area is caused by liberation of residual tensile on welding area, the decrement of dislocation density or dislocation reposition on low energy and residual martensit that brittle on welding structure with decomposition so that welding toughness increase.

4.3. Fracture macro Photograph

Fracture macro photograph from four specimens is illustrated in the Picture 10.



Picture 10. Specimen crack photograph (a) without treatment, (b) Stress relief annealing 500⁰ C, (c) Stress relief annealing 600⁰ C, (d) Stress relief annealing 700⁰ C

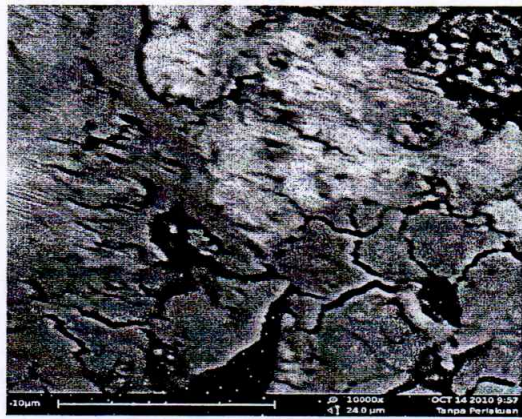
In Picture 10. (a), it shows the form of brittle crack. Brittle crack is shown by granular crack surface (granular) and bright. Crack creeping on welding connection creeps quickly and cause fracture.

In the Picture 10.(b), (c) and (d), it shows the form of fracture in tough; it means the influence of stress relief annealing treatment toward welding connection is visible. Toughness fracture gives fibrous characteristic (fibrous) and dark (dull). Tough fracture is preferred because tough material commonly stronger and give caution first before deflection.

4.4. Fracture photograph (Fraktografi)



a. Stress relief annealing 500⁰ C,



b. (a) without treatment

Picture 11. Fracture Photograph with SEM

The result of observation for surface fracture as the seen that the treatment with 500C have the ductile fracture because in the fracture have dimple, for specimen without treatment have cleavage fracture (brittle fracture)

5. CONCLUSION

From the result of this experiment, fatigue crack creeping conducted, it can be concluded that by stress relief annealing treatment in temperature of 500⁰ C by 60 minutes can give the best resistance of fatigue crack creeping rate on welding area.

REFERENCES

1. Broek, D. 1987. *Elementary Engineering Fracture Mechanics*. 4th ed. Martinus Nihhoff Pubs. Nederland.
2. Dieter, GE. 1987. *Metallurgi of Mechanic*. Edisi 3 jilid 1, Erlangga.
3. Harrison, P.L. dan Farrar, R.A. 1981. *Influence of Oxygen-rich Inclusions on the $\gamma \rightarrow \alpha$ Phase Transformation in High Strength Low Alloy (HSLA) Steel Weld Metals*. Journal of Material Science. 16. 2218-2226.
4. Ilman, M.N, and Sukrisno, R., 2005. *Toughness treatment and Fracture Mechanic in SAW Spiral Pipes API 5L X 52 with Stress Relief heat Treatment*. UGM. Yogyakarta.
5. Iscor Ltd. 2000. *Hot Rolled Strip for line pipe*. PO Box 2, Vanderbijlpark.
6. Miskat, I. and Subeki, N., 2008. *Stress Relief Annealing for SAW product in API 5L X52 Steel to Fracture Mechanic and Micro Structure*. UMM. Malang.
7. Mittal Steel South Africa. 1995. *Hot Rolled Strip For Line Pipe*. PO Box 2, Vanderbijlpark 1900.
8. Purwaningrum, Yustiningsih. 2005. *The Influaence of Fluks Index to Micro Structure, Toughness and Fracture Mechanic for Submerged Acd Welding Hight Steel Low Alloy (HSLA)*. UGM. Yogyakarta.
9. Radaj, D. 1992. *Heat Effects of Welds*. Springer Verlag. Berlin.
10. Sonawan, H dan Suratman, R. 2003. *Metal Welding*. CV. Alfabeta. Bandung.
11. Surdia, T, M.S. Met. E dan Saito, S. 1995. *Engineering Mataterial Science*. PT. Pradnya Paramita. Jakarta
12. Wiryosumarto, H dan Okumura, T. 2000. *Metal Welding Tecnologi*. PT. Pradnya Paramita. Jakarta